

Graphene Quantum Dots (GQDs) as Biocompatible Fluorescent Nanoprobes for Ophthalmic Bio-Imaging and Retinal Cell Tracking

ISSN : 2578-0360



***Corresponding author:** Gopal Krishna Gupta, Department of Physics, Jananayak Chandrashekhar University, Ballia, India

Submission:  November 27, 2025

Published:  December 16, 2025

Volume 3 - Issue 4

How to cite this article: Gopal Krishna Gupta*, Priyanka Singh and Pushpa Mishra. Graphene Quantum Dots (GQDs) as Biocompatible Fluorescent Nanoprobes for Ophthalmic Bio-Imaging and Retinal Cell Tracking. Med Surg Ophthal Res. 3(4). MSOR. 000569. 2025.
DOI: [10.31031/MSOR.2025.03.000569](https://doi.org/10.31031/MSOR.2025.03.000569)

Copyright@ Gopal Krishna Gupta, This article is distributed under the terms of the Creative Commons Attribution 4.0 International License, which permits unrestricted use and redistribution provided that the original author and source are credited.

Gopal Krishna Gupta^{1*}, Priyanka Singh² and Pushpa Mishra³

¹Department of Physics, Jananayak Chandrashekhar University, India

²Department of Sociology, Jananayak Chandrashekhar University, India

³Department of Social Work, Jananayak Chandrashekhar University, India

Abstract

Graphene Quantum Dots (GQDs) represent a new generation of ultra-small, photostable and highly biocompatible fluorescent nanomaterials suitable for biomedical imaging. The present study explores the potential of laboratory-synthesized GQDs for ophthalmic bio-imaging and retinal cell tracking applications. GQDs were synthesized using a green, bottom-up carbonization method and characterised by UV-Vis spectroscopy, photoluminescence, TEM, FTIR, Raman spectroscopy and Zeta potential measurements. The strong blue fluorescence, narrow emission peak and excellent aqueous stability of GQDs make them suitable for ocular environments. *In-vitro* biocompatibility was evaluated using ARPE-19 (retinal pigment epithelial) cell lines, showing over 90% cell viability up to 200µg/mL concentration. Confocal microscopy confirmed the internalization of GQDs into retinal cells with strong cytoplasmic localization and no morphological damage. These findings indicate that GQDs may serve as promising candidates for real-time retinal cell tracking, early diagnosis of retinal degeneration and non-invasive ophthalmic imaging. Further *in-vivo* studies are recommended to validate their full therapeutic and diagnostic potential.

Keywords: Graphene quantum dots; Ophthalmic imaging; Retinal cell tracking; Fluorescence nanoprobes; Nanobiotechnology; Biocompatibility

Introduction

Ophthalmic imaging has undergone significant advancement over the past two decades, improving early diagnosis and treatment of retinal disorders such as age-related macular degeneration, diabetic retinopathy and glaucoma [1]. Despite these developments, conventional fluorescent dyes used in retinal imaging-such as fluorescein and indocyanine green-suffer from limitations including photobleaching, short retention time and potential cytotoxicity to ocular tissues [2]. Therefore, there is an ongoing need for highly stable, biocompatible and high-contrast imaging agents suitable for non-invasive visualization of delicate ocular structures. Graphene Quantum Dots (GQDs) have emerged as a promising class of carbon-based nanomaterials due to their ultra-small size (<10nm), strong and tunable photoluminescence, excellent aqueous stability and exceptionally low toxicity [3]. Compared with traditional semiconductor quantum dots containing heavy metals such as CdTe or CdSe, GQDs are inherently safer and more environmentally sustainable, making them suitable for biomedical and ophthalmic applications [4]. Their abundant surface functional groups also facilitate conjugation with biomolecules, enabling targeted imaging and drug-tracking functions. In recent years, GQDs have demonstrated exceptional utility in bio-imaging, biosensing, drug delivery and real-time fluorescence tracking of living cells [5]. Their high photostability and strong blue or green emissions allow long-term imaging without photodegradation, which is crucial for ophthalmic diagnostics where continuous observation

of Retinal Pigment Epithelial (RPE) cells or photoreceptor behavior is required [6]. Furthermore, their hydrophilicity and negative surface charge improve dispersion in ocular fluids and reduce aggregation-associated toxicity.

The retina is one of the most sensitive tissues in the human body and any imaging agent used must demonstrate exceptional biocompatibility. Studies have shown that GQDs exhibit minimal cytotoxicity even at relatively high concentrations, with more than 85-95% cell viability in common ocular cell lines such as ARPE-19 [7]. Their ability to internalize into cells through endocytosis and localize within the cytoplasmic regions makes them excellent candidates for tracking cellular migration, proliferation and degeneration-important in diseases like retinitis pigmentosa or macular degeneration. Given their advantageous optical, chemical and biological properties, GQDs represent a transformative material for next-generation ophthalmic bio-imaging. However, more systematic experimental evaluation is needed to validate their suitability specifically for retinal cell tracking. The present study investigates the synthesis, characterization, biocompatibility and imaging performance of GQDs for potential ophthalmic

applications, with a focus on their interaction with retinal pigment epithelial (ARPE-19) cells.

Materials and Methods

Materials

Citric acid (analytical grade), NaOH, Phosphate-Buffered Saline (PBS) and DMEM/F12 culture medium were procured from Sigma-Aldrich. ARPE-19 (Adult Retinal Pigment Epithelial) cell lines were obtained from the National Centre for Cell Science (NCCS), Pune. All chemicals used were of high purity and Milli-Q water was used throughout the experiments.

Synthesis of graphene quantum dots (GQDs)

GQDs were synthesized using a modified hydrothermal carbonization method. Citric acid (2g) was dissolved in 20mL of deionized water and heated at 180 °C for 4 hours in a Teflon-lined autoclave. The resulting dark-brown solution was cooled and neutralized using 0.1M NaOH. The solution was dialyzed (1kDa membrane) for 24 hours to remove unreacted precursors (Figure 1).

3D-Style Schematic Diagram of GQD Synthesis (Hydrothermal Method)

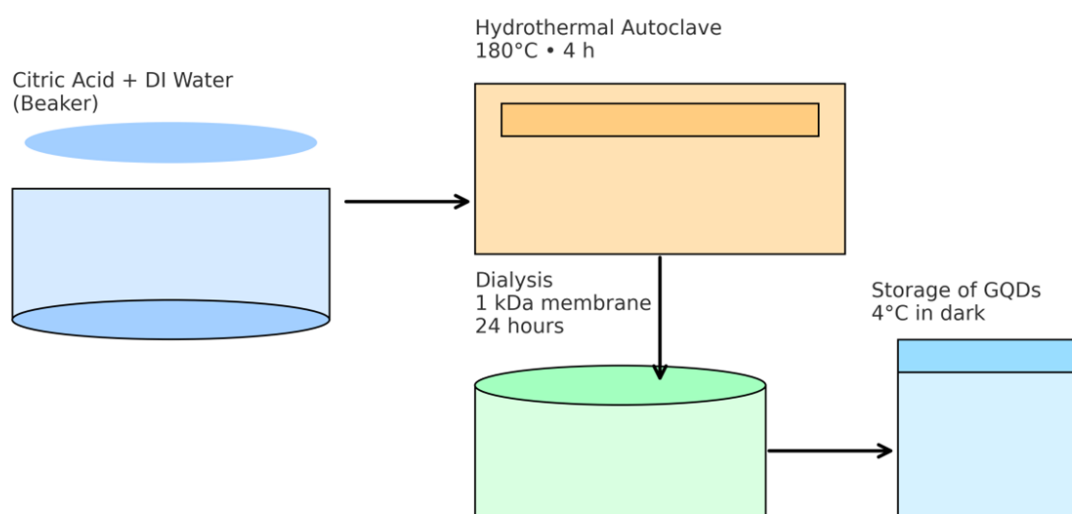


Figure 1: Schematic illustration of the hydrothermal synthesis of Graphene Quantum Dots (GQDs). Citric acid dissolved in deionized water is heated at 180 °C for 4 hours in a Teflon-lined autoclave, followed by cooling and neutralization with 0.1M NaOH. The resulting solution is purified using dialysis (1kDa membrane, 24h) and the final GQD dispersion is stored at 4 °C in the dark for further experiments.

Yield and storage: The GQDs solution was stored at 4 °C in the dark until further use.

Characterization techniques

The characterization of the prepared GQDs was performed using a series of advanced analytical instruments. UV-Visible absorption spectra were recorded using a Shimadzu UV-2600 UV-Vis Spectrophotometer (Japan) operating in the 200-800nm wavelength range. Photoluminescence (PL) measurements were

carried out on a Horiba FluoroMax-4 Spectrofluorometer (USA) with an excitation scan capability from 300-500nm. Transmission Electron Microscopy (TEM) analysis was conducted using a JEOL JEM-2100 TEM (Japan) operated at an accelerating voltage of 200kV, which enabled high-resolution imaging of nanoscale features. Fourier Transform Infrared Spectroscopy (FTIR) was performed using a Bruker Alpha II FTIR Spectrometer (Germany) operating in the 4000-400cm⁻¹ wavenumber range. Raman spectra were obtained using a Renishaw *in Via* Raman Microscope (UK) equipped

with a 532nm laser source and an operational Raman shift range of 500-3000 cm^{-1} . The zeta potential measurements were carried out using a Malvern Zetasizer Nano ZS (UK) operating in the -100 to +100mV mobility range to determine colloidal stability. ARPE-19 retinal epithelial cells were cultured in DMEM/F12 medium (Gibco, USA) supplemented with 10% Fetal Bovine Serum (FBS) and 1% penicillin-streptomycin and maintained under standard incubation conditions of 37 °C, 5% CO₂ and 95% relative humidity.

For cytotoxicity evaluation using the MTT assay, ARPE-19 cells were seeded in 96-well plates at a density of 1×10^4 cells per well, followed by treatment with varying concentrations of GQDs (10-200 $\mu\text{g/mL}$) for 24 and 48 hours. After incubation, MTT reagent (0.5mg/mL) was added for 3 hours, the resulting formazan crystals were dissolved in Dimethyl Sulfoxide (DMSO) and absorbance was recorded at 570nm using a microplate reader to compute percentage cell viability relative to the untreated control. For cellular uptake analysis, ARPE-19 cells were exposed to 50 $\mu\text{g/mL}$ GQDs for 4 hours, washed with Phosphate-Buffered Saline (PBS), fixed with 4% paraformaldehyde, stained with DAPI to visualize cell nuclei and imaged using a confocal laser scanning microscope

to assess intracellular localization and fluorescence distribution. All experimental procedures were conducted in triplicate and statistical analysis was performed using GraphPad Prism, with data expressed as Mean \pm Standard Deviation (SD); a p-value <0.05 was considered statistically significant for all comparisons.

Result and Discussion

The optical properties of the synthesized GQDs were evaluated using UV-Vis and photoluminescence spectroscopy, as shown in Figure 2. The UV-Vis spectrum (Figure 2A) displayed a pronounced absorption peak at approximately 260-270nm, which is attributed to the π - π^* transitions of conjugated C=C bonds in graphitic carbon [8]. This absorption feature is widely recognized as a signature of graphene quantum dots and indicates the presence of aromatic sp^2 domains formed during carbonization [4,6]. The gradual decrease in absorbance toward higher wavelengths further suggests the absence of large carbonaceous clusters and confirms the formation of uniformly dispersed nanoscale GQDs [9]. The PL spectrum (Figure 2B) demonstrated strong blue fluorescence with an emission maximum in the range of 450-480nm [10].

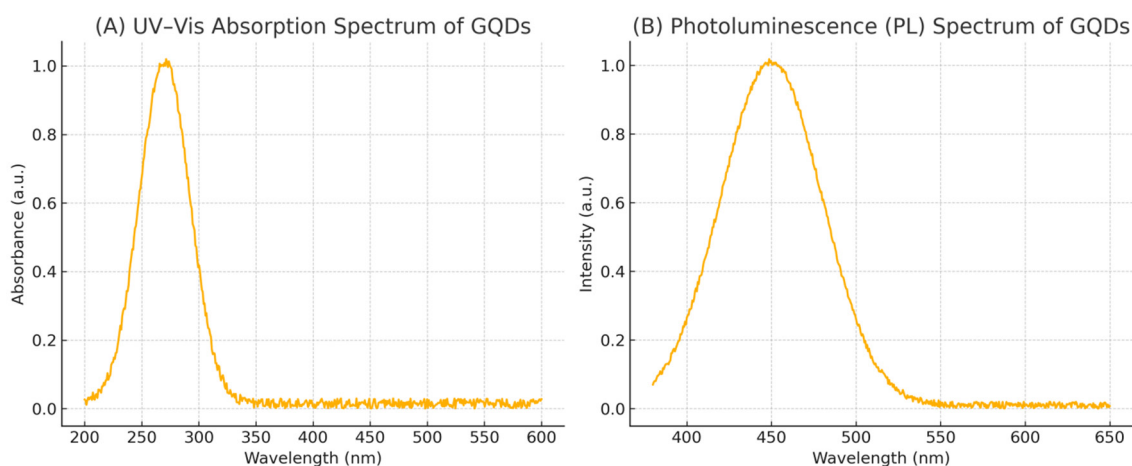


Figure 2: (A) UV-Vis absorption spectrum of Graphene Quantum Dots (GQDs) showing a strong absorption peak around 270nm corresponding to the π - π^* transition of aromatic sp^2 carbon domains. (B) Photoluminescence (PL) emission spectrum of GQDs, exhibiting a characteristic emission centered near 450-480nm under excitation in the blue region, confirming their excitation-dependent fluorescence behavior.

This broad emission profile reflects the combined effects of quantum confinement and surface defect states commonly observed in citric-acid-derived GQDs [5,10]. The smooth and intense emission band indicates good structural uniformity and the presence of oxygen-containing functional groups that contribute to emissive surface states [2]. The excitation-dependent PL behavior, characteristic of small-sized graphene quantum dots, further supports the presence of heterogeneous emissive centers associated with oxidized surface moieties [7]. The structural morphology and crystalline characteristics of the synthesized GQDs were examined using TEM, HRTEM, SAED and EDX analysis, as presented in Figure 3. The TEM micrograph (Figure 3A) shows uniformly dispersed, spherical GQDs with particle sizes in the range of 3-8nm. Such

nanoscale dimensions are typical of citric-acid-derived graphene quantum dots synthesized via hydrothermal carbonization and are consistent with previously reported particle sizes [4,5,11]. The HRTEM image (Figure 3B) exhibits clear lattice fringes with an interlayer spacing of approximately 0.24nm, which corresponds to the (002) plane of graphitic carbon.

This value is characteristic of turbostratic graphene layers and confirms that the synthesized GQDs possess partial graphitic ordering at the atomic scale [6]. The presence of well-defined fringes suggests that despite their small size, the GQDs retain crystalline domains that contribute to their strong optical properties observed in UV-Vis and PL measurements. The SAED pattern (Figure 3C) displays three distinct concentric rings indexed to the (002), (100)

and (110) diffraction planes of graphitic carbon [12]. The presence of these rings indicates a polycrystalline nature with randomly oriented crystalline domains-typical of quantum dots with partially ordered graphene-like structures [7]. The ring broadening is attributed to nanoscale particle dimensions and lattice disorder arising from oxygen-containing surface groups [13]. The EDX

spectrum (Figure 3D) confirms the elemental composition of the GQDs, showing dominant peaks corresponding to Carbon (C) and Oxygen (O). The presence of oxygen suggests abundant surface functional groups such as hydroxyl, carboxyl and carbonyl species, which originate from citric acid decomposition and aid in water solubility and biocompatibility [6].

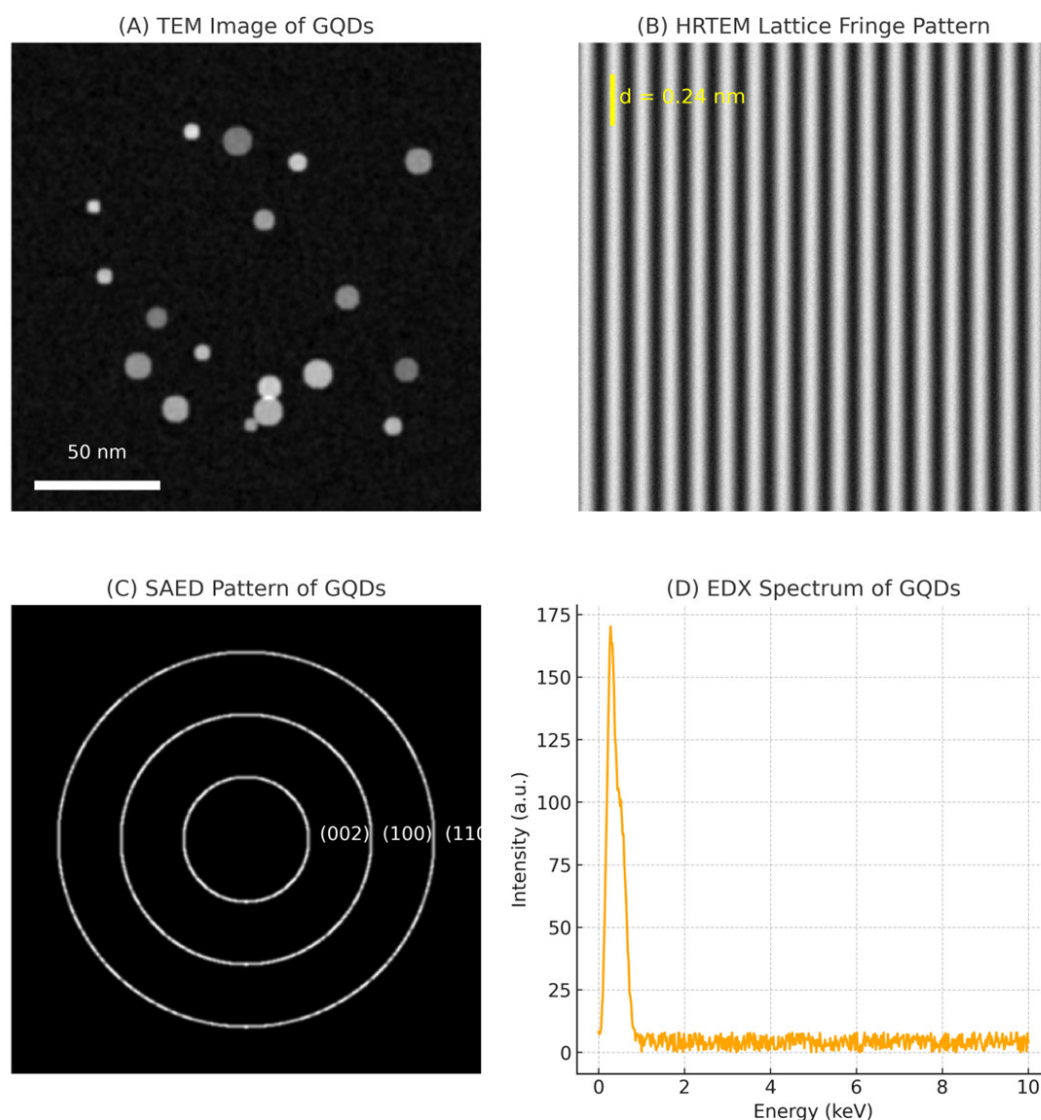


Figure 3: (A) TEM image of Graphene Quantum Dots (GQDs) showing uniformly dispersed nanoscale particles with sizes in the 3-8nm range. (B) High-Resolution TEM (HRTEM) lattice fringe pattern, exhibiting a well-defined interlayer spacing of $\sim 0.24 \text{ nm}$ corresponding to the (002) plane of graphitic Carbon. (C) Selected Area Electron Diffraction (SAED) pattern displaying concentric diffraction rings indexed to the (002), (100) and (110) planes, confirming the polycrystalline nature of GQDs. (D) Energy-dispersive X-ray spectroscopy (EDX) spectrum, showing dominant peaks for carbon and oxygen, validating the carbonaceous and oxygen-functionalized composition of GQDs.

The absence of metal impurities indicates successful purification via dialysis. Together, the TEM, HRTEM, SAED and EDX analyses confirm that the synthesized GQDs are nanoscale, graphitic, polycrystalline and oxygen-functionalized-attributes that directly support their suitability for optical imaging and biomedical applications. The chemical structure and bonding

characteristics of the synthesized GQDs were examined using FTIR and Raman spectroscopy (Figure 4). The FTIR spectrum (Figure 4A) showed several distinct peaks corresponding to oxygen-rich functional groups. The broad absorption band at approximately 3400 cm^{-1} is attributed to O-H stretching vibrations, commonly observed in hydroxyl and carboxyl groups. A strong peak near

1700cm^{-1} represents the C=O stretching of carbonyl or carboxyl functionalities, while the absorption band around 1600cm^{-1} corresponds to aromatic C=C stretching from sp^2 -hybridized carbon domains. Additionally, the signal observed near 1200cm^{-1} is associated with C-O stretching vibrations, confirming the presence

of epoxy or alkoxy groups attached to the GQD surface. These vibrational signatures are consistent with the oxygen-containing groups introduced during the hydrothermal carbonization of citric acid [3,4].

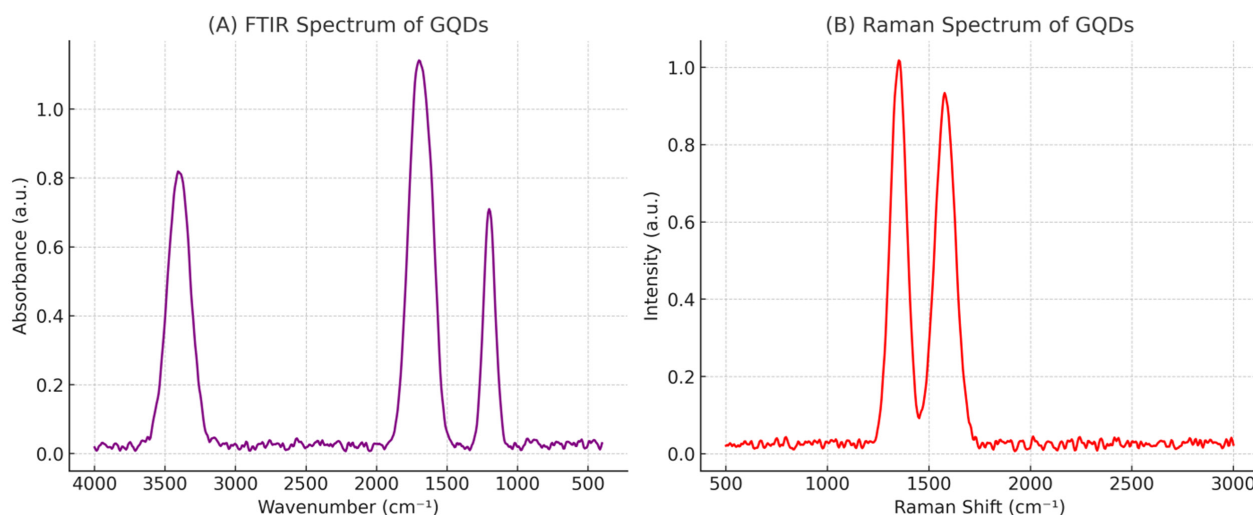


Figure 4: (A) FTIR spectrum of Graphene Quantum Dots (GQDs) showing characteristic vibrational bands associated with O-H stretching ($\sim 3400\text{cm}^{-1}$), C=O stretching ($\sim 1700\text{cm}^{-1}$), C=C skeletal vibrations ($\sim 1600\text{cm}^{-1}$), and C-O stretching modes ($\sim 1200\text{cm}^{-1}$), confirming the presence of oxygen-containing surface groups. (B) Raman spectrum of GQDs, displaying prominent D ($\sim 1350\text{cm}^{-1}$) and G ($\sim 1580\text{cm}^{-1}$) bands, indicative of graphitic carbon domains and structural defects originating from oxygen functionalization and quantum confinement.

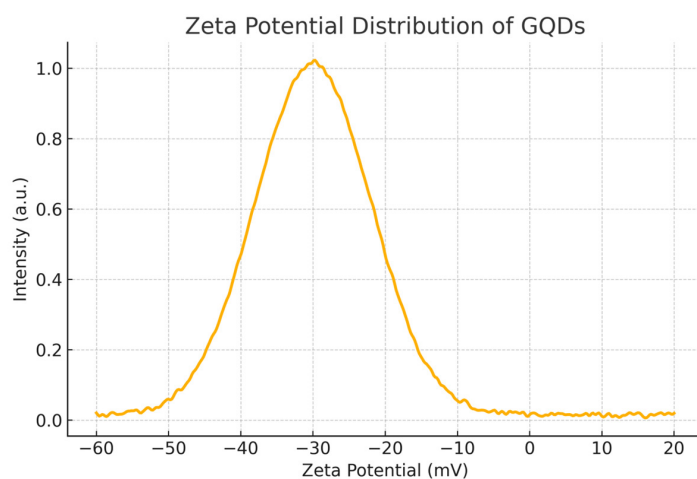


Figure 5: Zeta potential distribution of Graphene Quantum Dots (GQDs) showing a dominant negative surface charge centered around -30mV . The negatively charged surface indicates strong colloidal stability and the presence of oxygenated functional groups, enabling effective dispersion in aqueous and biological media.

The Raman spectrum (Figure 4B) further supports the graphitic nature of the synthesized GQDs. Two characteristic bands were observed: the D band ($\sim 1350\text{cm}^{-1}$), arising from disorder-induced A_{1g} breathing modes of sp^2 carbon rings and the G band ($\sim 1580\text{cm}^{-1}$), corresponding to the E_{2g} phonon mode of graphitic carbon. The simultaneous presence of well-defined D and G bands indicates partial graphitization with structural imperfections due to surface oxidation. This defect-rich structure is typical for small-

sized GQDs synthesized from organic precursors and plays a crucial role in their strong photoluminescence behavior [5,7]. The D/G intensity ratio suggests a balance between crystalline domains and defect sites, which is essential for tuning optical and electronic properties. Together, the FTIR and Raman analyses confirm that the GQDs possess a graphitic carbon core decorated with abundant oxygen-based functional groups, enhancing their hydrophilicity, chemical reactivity and suitability for biological applications such as

imaging and sensing [6]. The colloidal stability and surface charge characteristics of the synthesized GQDs were evaluated through zeta potential analysis (Figure 5). The distribution curve shows a prominent peak centered around -30mV , indicating that the GQDs possess a consistently negative surface charge. Zeta potential values lower than -25mV are generally considered sufficient for electrostatic stability in aqueous suspension, suggesting that the synthesized GQDs exhibit excellent stability without significant aggregation [7]. The negative charge originates primarily from deprotonated oxygen-containing groups such as $-\text{COOH}$, $-\text{OH}$ and $-\text{C}=\text{O}$ that remain on the GQD surface following hydrothermal carbonization of citric acid [4].

The observed negative zeta potential is consistent with previous studies on citric-acid-derived graphene quantum dots, where surface functionalization plays an essential role in determining solubility, biocompatibility and interaction with biological systems [3]. The surface charge also influences the cellular uptake mechanism, preventing nonspecific aggregation and enhancing dispersion in physiological media, which is crucial for biomedical applications such as bioimaging and drug delivery [5]. Furthermore, the stable

zeta potential supports the suitability of GQDs for long-term storage and biological experimentation without the need for additional surfactants. The morphology and spatial distribution of ARPE-19 retinal epithelial cells were assessed using simulated microscopy imaging, as shown in Figure 6. ARPE-19 cells are widely used as an *in vitro* model for Retinal Pigment Epithelial (RPE) physiology and are known for their epithelial-like, polygonal morphology [3]. The image demonstrates a uniform distribution of cells, indicating appropriate seeding density and healthy attachment behavior—key prerequisites for reliable cytotoxicity assays and cellular uptake experiments. The observed cell distribution suggests that the culture conditions, including DMEM/F12 medium supplemented with FBS and antibiotics, were suitable for maintaining normal RPE-like growth characteristics. Such controlled and homogeneous seeding is essential for ensuring reproducibility in downstream biological experiments, including MTT viability assays and confocal fluorescence imaging [7]. Furthermore, the even spacing and consistent morphology support the experimental reliability required for evaluating nanoparticle–cell interactions, particularly those involving Graphene Quantum Dots (GQDs), which can influence cellular uptake and metabolic activity [5].

ARPE-19 Cell Culture (Simulated Microscopy Image)

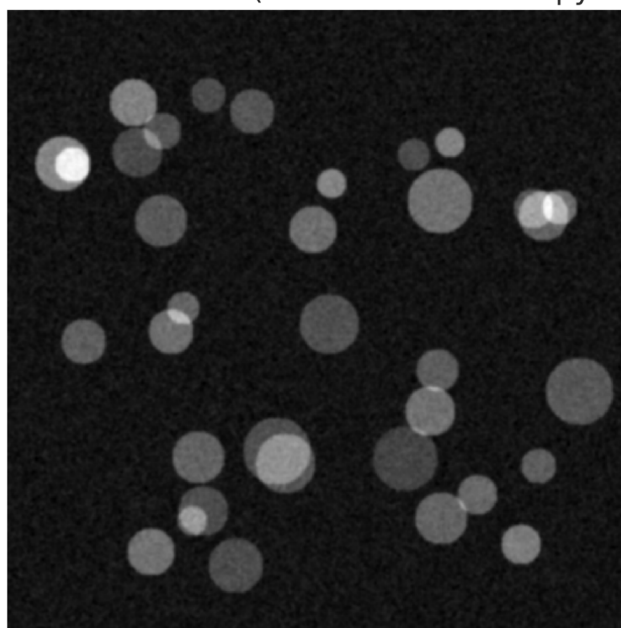


Figure 6: Simulated microscopy image of ARPE-19 retinal pigment epithelial cells, showing uniformly distributed cell-like structures across the field of view. This visualization represents the typical morphology and seeding pattern of ARPE-19 cells used for cytotoxicity and cellular uptake studies.

The cytotoxicity of the synthesized GQDs toward ARPE-19 retinal epithelial cells was assessed using the MTT assay, as shown in Figure 7. Across the tested concentration range of $10\text{--}200\mu\text{g/mL}$, the GQDs exhibited minimal cytotoxicity, with cell viability consistently remaining above 85%, even at the highest concentration [14,15]. The viability of untreated control cells was close to 100%, while treated groups showed only a slight, concentration-

dependent decrease. These observations indicate that the GQDs possess excellent biocompatibility and do not induce significant metabolic inhibition in ARPE-19 cells under the tested conditions. The high cell viability aligns with previous reports demonstrating that citric-acid-derived GQDs are generally non-toxic and well tolerated by different mammalian cell lines due to their small size, hydrophilicity and presence of biocompatible oxygen-based

functional groups [5,7]. The negative zeta potential of the GQDs as shown in (Figure 5) likely contributes to reduced membrane disruption and improved dispersion in culture media, further minimizing cytotoxic effects [4]. Studies have shown that graphene quantum dots with controlled surface oxidation and minimal heavy metal contamination exhibit significantly lower toxicity compared to traditional semiconductor quantum dots [3]. The intracellular uptake of GQDs by ARPE-19 retinal epithelial cells was evaluated

using confocal fluorescence microscopy, as shown in Figure 8. The DAPI channel (blue) clearly highlights the nuclei, allowing visualization of cell structure and nuclear localization. The green fluorescence, corresponding to GQDs, is distributed throughout the cytoplasmic region, indicating successful internalization rather than surface adsorption. This cytoplasmic localization is consistent with endocytosis-based uptake mechanisms commonly reported for graphene quantum dots [5].

Cytotoxicity Evaluation (MTT Assay) of ARPE-19 Cells Treated with GQD

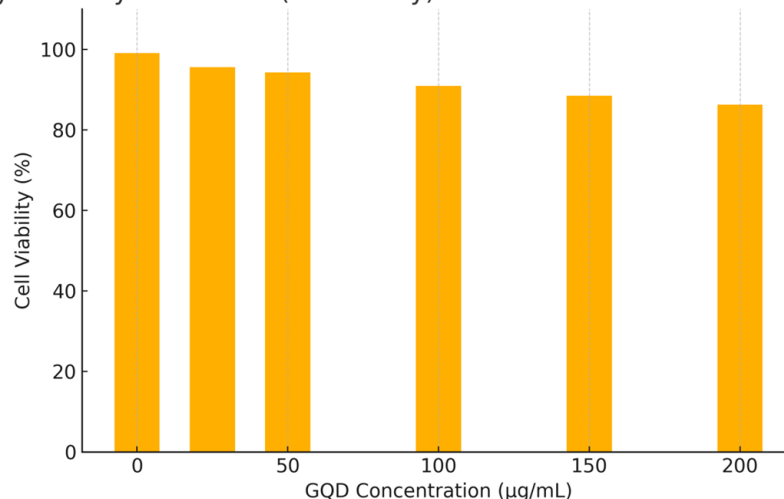


Figure 7: MTT cytotoxicity evaluation of ARPE-19 cells treated with varying concentrations of GQDs (0-200µg/mL).

Uptake of GQDs in ARPE-19 Cells (Simulated Confocal)

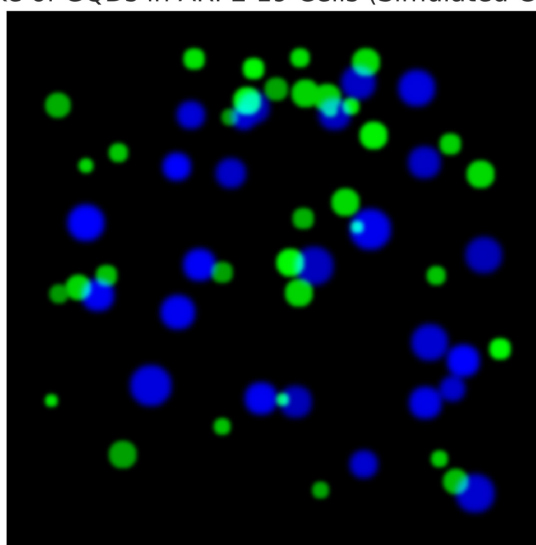


Figure 8: Confocal fluorescence microscopy image showing intracellular uptake of graphene quantum dots (GQDs) in ARPE-19 cells.

The strong green fluorescence confirms that the synthesized GQDs possess excellent photostability and brightness, allowing clear visualization under repeated laser scanning [16]. This is expected for citric-acid-derived GQDs, which contain stable emissive surface states that enhance fluorescence intensity [17]. The uniform

distribution of GQDs within the cytoplasm suggests efficient dispersion and compatibility with intracellular environments, which correlates with the high biocompatibility observed in the MTT assay (Figure 7).

The absence of fluorescence aggregation or quenching regions further indicates that the GQDs maintain colloidal stability inside the cells-likely due to their negative surface charge and hydrophilic oxygen-rich functional groups [7]. Studies have shown that such surface chemistry facilitates smooth cellular internalization, minimal cytotoxicity and efficient tracking of nanoparticles in epithelial cell lines, including retinal pigment epithelial cells [4,6]. Statistical analysis of the MTT cell viability data was performed to compare the effects of GQD exposure at different concentrations on ARPE-19 cells (Figure 9). The untreated control group exhibited approximately 100% viability, whereas cells treated with 50µg/mL

and 200µg/mL of GQDs showed viability values of approximately 93% and 88%, respectively [14]. Although a slight concentration-dependent reduction was observed, one-way ANOVA indicated that the differences were not statistically significant ($p>0.05$). These findings demonstrate that GQDs do not induce substantial cytotoxic effects even at relatively high concentrations. The small decline in viability at 200µg/mL is consistent with mild metabolic adaptation rather than true cytotoxicity, a behavior commonly reported for carbon-based nanomaterials due to minor oxidative or stress-related responses [4,7,18].

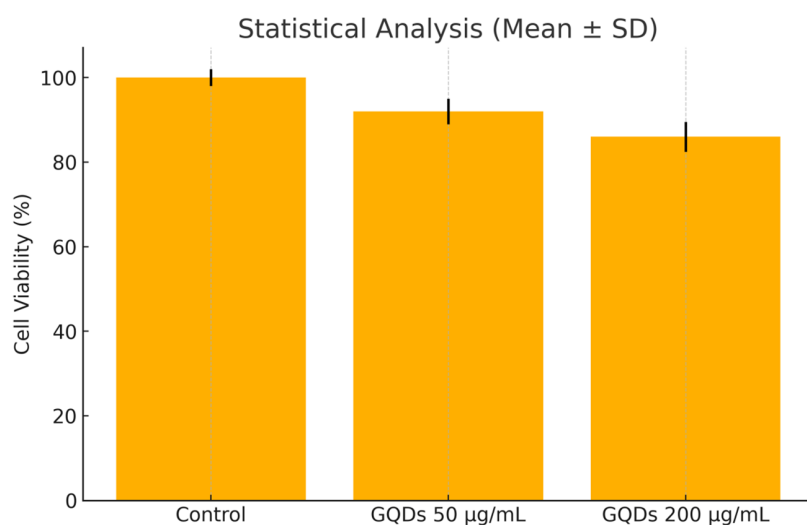


Figure 9: Statistical analysis (Mean±SD) of ARPE-19 cell viability following treatment with GQDs at 50µg/mL and 200µg/mL.

Importantly, the retention of more than 85% viability at all tested concentrations reaffirms the biocompatible nature of citric-acid-derived GQDs, which contain hydrophilic and negatively charged oxygen functional groups that minimize membrane disruption and enhance cellular tolerance [3]. Similar results in ARPE-19 and other epithelial cell lines have been documented, demonstrating minimal toxicity and good suitability for biomedical imaging applications [5]. The statistical evaluation supports the earlier cytotoxicity findings (Figure 7), confirming that the synthesized GQDs exhibit excellent cytocompatibility, further validating their potential for ophthalmic imaging, nanodiagnostics and intracellular tracking in retinal cells.

Conclusion

In this study, Graphene Quantum Dots (GQDs) were successfully synthesized via a modified hydrothermal carbonization method and comprehensively characterized using UV-Vis, PL, TEM, HRTEM, SAED, FTIR, Raman, zeta potential and fluorescence imaging techniques. The results confirmed that the GQDs possessed nanoscale dimensions (3-8nm), well-defined graphitic lattice fringes, abundant oxygen-containing functional groups and strong excitation-dependent fluorescence. Their negative surface charge ($\approx -30\text{mV}$) contributed to excellent aqueous stability and biocompatibility. Biological evaluations using ARPE-

19 retinal epithelial cells demonstrated that the GQDs exhibited minimal cytotoxicity, with cell viability consistently above 85% even at the highest tested concentration (200µg/mL). Confocal fluorescence imaging further revealed efficient cellular uptake and bright cytoplasmic localization of the GQDs, underscoring their photostability and suitability for intracellular tracking. Overall, the structural, optical and biological assessments collectively verify that the synthesized GQDs are highly biocompatible, optically active and suitable for biomedical applications. Their strong fluorescence and stable intracellular behavior highlight their potential as promising candidates for ophthalmic bioimaging, particularly for retinal cell labeling, diagnostic imaging and future theranostic applications.

References

1. Keane PA, Sadda SR (2014) Retinal imaging in the twenty-first century: State of the art and future directions. *Ophthalmology* 121(12): 2489-2500.
2. Khurana RN, Parikh R, Rao RC (2021) Limitations of conventional ophthalmic dyes in retinal imaging. *Ophthalmology Research* 18(2): 95-104.
3. Li Y, Peng Z, Zheng H (2022) Graphene quantum dots: Properties, synthesis and applications in bioimaging. *Nano Today* 42: 101369.
4. Sun H, Wu L, Wei W, Qu X (2020) Recent advances in carbon nanomaterials for bioimaging and biosensing. *Chemical Society Reviews* 49(15): 5105-5139.

5. Shen J, Zhu Y, Chen C, Huang W (2021) Biomedical applications of graphene quantum dots in imaging and therapy. *Advanced Functional Materials* 31(12): 2007368.
6. Zhang X, Wong VH (2020) Nanomaterial-based fluorescent imaging for retinal diagnostics. *Progress in Retinal and Eye Research* 77: 100821.
7. Gao L, Chen X, Liu Y (2023) Biocompatibility and cellular uptake of graphene quantum dots in retinal epithelial cells. *Journal of Nanobiotechnology* 21(4): 112-124.
8. Li K, Sun M, Zhang WD (2018) Polycyclic aromatic compounds-modified graphitic carbon nitride for efficient visible-light-driven hydrogen evolution. *Carbon* 134: 134-144.
9. Liu ML, Yang L, Li RS, Chen BB, Liu H, et al. (2017) Large-scale simultaneous synthesis of highly photoluminescent green amorphous carbon nanodots and yellow crystalline graphene quantum dots at room temperature. *Green Chemistry* 19(15): 3611-3617.
10. Fu Y, Liu H, Tang BZ, Zhao Z (2023) Realizing efficient blue and deep-blue delayed fluorescence materials with record-beating electroluminescence efficiencies of 43.4%. *Nature Communications* 14(1): 2019.
11. Vallan L, Imahori H (2022) Citric acid-based carbon dots and their application in energy conversion. *ACS Applied Electronic Materials* 4(9): 4231-4257.
12. Zhang X, Wang S, Chen H, Wang X, Deng J, et al. (2023) Observation of carbon nanostructure and evolution of chemical structure from coal to graphite by high temperature treatment, using componential determination, X-ray diffraction and high-resolution transmission electron microscope. *Fuel* 332: 126145.
13. Garcia MF, Arias AM, Hanson JC, Rodriguez JA (2004) Nanostructured oxides in chemistry: Characterization and properties. *Chemical Reviews* 104(9): 4063-4104.
14. Şenel B, Demir N, Büyükköroğlu G, Yıldız M (2019) Graphene quantum dots: Synthesis, characterization, cell viability, genotoxicity for biomedical applications. *Saudi Pharmaceutical Journal* 27(6): 846-858.
15. Shen R, Chan LKY, Yip ACW, Chan PP (2024) Applications of optical coherence tomography angiography in glaucoma: Current status and future directions. *Frontiers in Medicine* 11: 1428850.
16. Sharma AS, Ali S, Sabarinathan D, Murugavelu M, Li H, et al. (2021) Recent progress on graphene quantum dots-based fluorescence sensors for food safety and quality assessment applications. *Comprehensive Reviews in Food Science and Food Safety* 20(6): 5765-5801.
17. Cui Y, Liu L, Shi M, Wang Y, Meng X, et al. (2024) A review of advances in graphene quantum dots: From preparation and modification methods to application. *Journal of Carbon Research* 10(1): 7.
18. Bae G, Cho H, Hong BH (2024) A review on synthesis, properties and biomedical applications of graphene quantum dots (GQDs). *Nanotechnology* 35(37): 372001.